

performed the best for suctions of 10, 33, and 100 kPa and Rawls et al. (1982) PTF performed the best for suction of 1500 kPa.

Table 3. Evaluation indices for point PTFs

Suction (kPa)	PTF	MSE	RMSE	R ²
10	Hall et al. (1977)	0.0047	0.069	0.724
	Gupta and Larson (1979)	0.0029	0.053	0.834
	Rawls et al. (1982)	0.0043	0.065	0.752
	Tomasella and Hodnett (1998)	0.0050	0.071	0.708
33	Gupta and Larson (1979)	0.0027	0.052	0.89
	Aina and Periaswamy (1985)	0.0039	0.062	0.85
	Beke and MacCormick (1985)	0.0052	0.072	0.80
	Tomasella and Hodnett (1998)	0.0034	0.058	0.87
100	Gupta and Larson (1979)	0.0033	0.057	0.84
	Rawls et al. (1982)	0.0043	0.065	0.79
	Tomasella and Hodnett (1998)	0.0063	0.079	0.70
	Reichert et al. (2009)	0.0202	0.142	0.69
1500	Hall et al. (1977)	0.0015	0.039	0.84
	Rawls et al. (1982)	0.0013	0.036	0.86
	Marique et al. (1991)	0.0015	0.039	0.84
	Dashtaki et al. (2010)	0.0017	0.041	0.82

The performance of using Gupta and Larson (1979) PTFs for suctions of 10, 33 and 100 kPa and Rawls et al. (1982) PTF for suction of 1500 kPa to estimate the SWCCs for three soils are shown in Figure 6. The properties of the three soils are summarized in Table 4. In Figure 6, the curve is obtained by best-fitting Fredlund and Xing (1994) equation (solid line) and van Genuchten (1980) equation (dotted line) to the four points. The PTFs provide good estimates of the water contents at 10, 33, 100 and 1500 kPa. Soils 2361 and 1360 are fine-grained soils while soil 4560 is a coarse-grained soil. Good estimate of the SWCC is obtained using the four points for the fine-grained soils (Soils 2361 and 1360) but the estimate of the SWCC for the coarse-grained soil (Soil 4560) is only good at suctions greater than 10 kPa. There is a big change in the SWCC for Soil 4560 from 0 to 10 kPa suction and it is reasonable to expect that the best-fitted Fredlund and Xing (1994) equation cannot provide a good estimate the SWCC in this suction range without any data points.

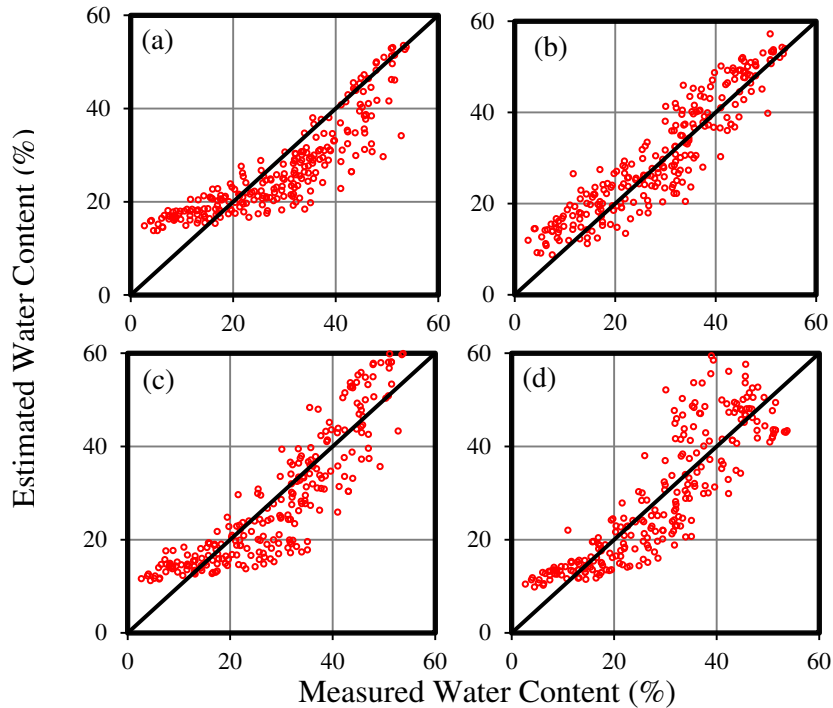


Figure 2. Measured and estimated water content using point PTFs at suction of 10 kPa: (a) Hall et al. (1977), (b) Gupta and Larson (1979), (c) Rawls et al. (1982), and (d) Tomasella and Hodnett (1998).

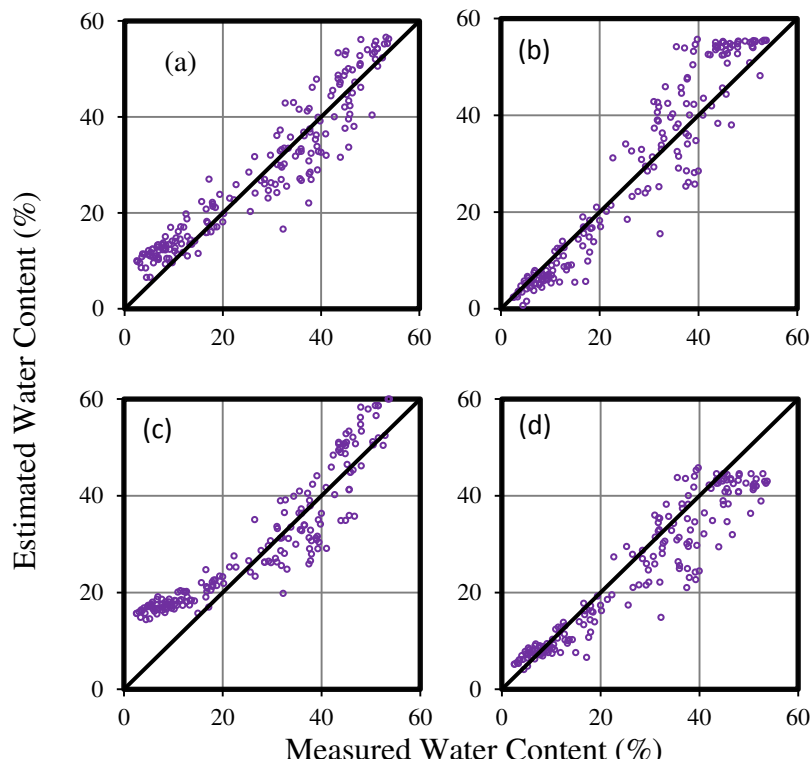


Figure 3. Measured and estimated water contents using point PTFs at suction of 33 kPa: (a) Gupta and Larson (1979), (b) Aina and Periaswamy (1985), (c) Beke and MacCormick (1985), and (d), Tomasella and Hodnett (1998).

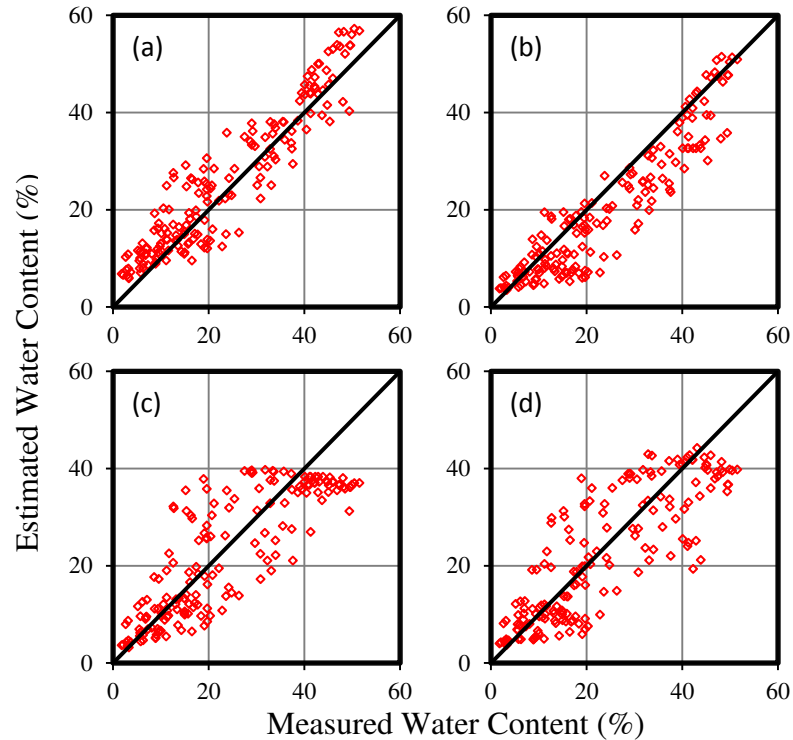


Figure 4. Measured and estimated water contents using point PTFs at suction of 100 kPa: (a) Gupta and Larson (1979), (b) Rawls et al. (1982), (c) Tomasella and Hodnett (1998), and (d) Reichert et al. (2009).

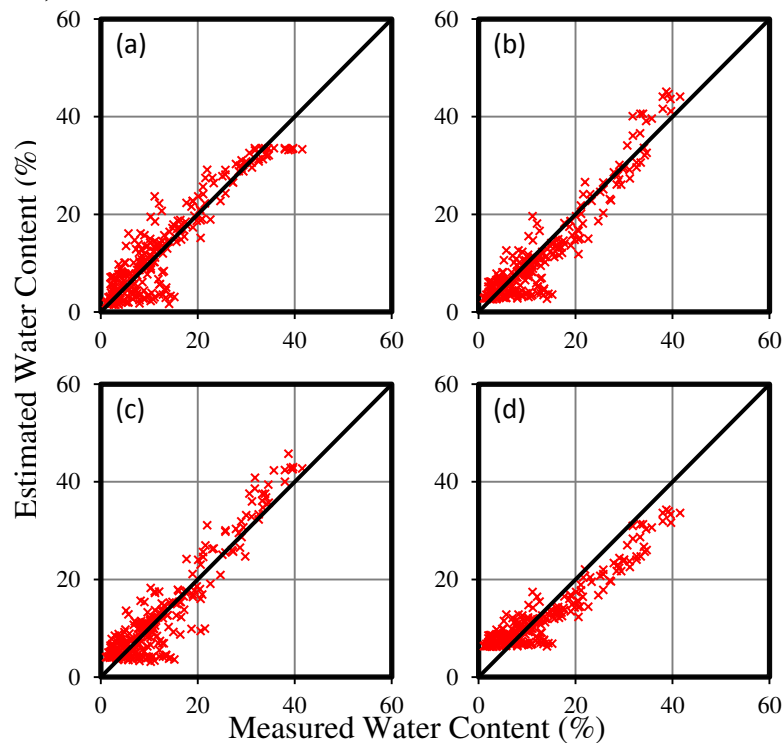


Figure 5. Measured and estimated water contents using point PTFs at suction of 1500 kPa: (a) Hall et al. (1977), (b) Rawls et al. (1982), (c), Marique et al. (1991), and (d) Dashtaki et al. (2010).

Table 4. Properties of three soils from UNSODA used for estimation of SWCC with four SWCC points from PTFs

Soil	Void Ratio	ρ_d (Mg/m ³)	Sa (%)	Si (%)	Cl (%)
2361	1.257	1.280	8.0	36.0	56.0
1360	0.813	1.500	15.7	40.8	43.5
4650	0.613	1.622	92.0	7.0	1.0

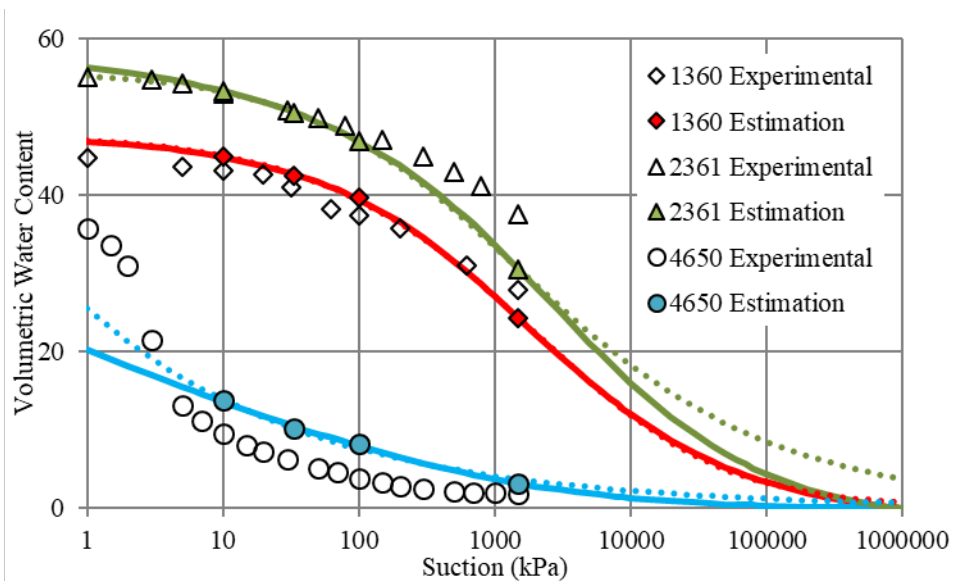


Figure 6. Estimation of SWCC using four estimated SWCC points from PTFs and Fredlund and Xing (1994) equation (solid line) and van Genuchten (1980) equation (dotted line).

CONCLUSION

Point pedo-transfer functions (PTFs) are commonly used in soil science and agriculture to estimate the water content at suctions of 10, 33, 100 and 1500 kPa. However, point PTFs are not commonly used in unsaturated soil mechanics. In this paper, a number of point PTFs (9 PTFs for 10 kPa, 15 PTFs for 33 kPa, 5 PTFs for 100 kPa and 18 PTFs for 1500 kPa) was evaluated using 60 soils from Andersson and Wiklert (1972), 60 soils from Jauhiainen (2004) and 130 soils from UNSODA (Nemes, et al., 2001). The evaluation results show that Gupta and Larson (1979) PTF performed well at suctions of 10, 33 and 100 kPa while Rawls et al. (1982) PTF performed well at suction of 1500 kPa. Using these point PTFs, a quick estimate of SWCC can be obtained using Gupta and Larson (1979) to estimate the water contents at suctions of 10, 33 and 100 kPa and Rawls et al. (1982) PTF to estimate the water content at suction of 1500 kPa as illustrated for three soils. The estimated SWCCs have a good agreement with the experimental SWCC for suctions between 10 and 1500 kPa. Such point PTFs provide an alternative method to obtain the SWCC and should be further explored in unsaturated soil mechanics.

REFERENCES

- Aina, P.O., and Perisawamy, S.P. (1985). "Estimating available water-holding capacity of western Nigerian soils from soil texture and bulk density, using core and sieved samples." *Soil Sci.*, 140, 55-58.
- Andersson, S., and Wiklert, P. (1972). "Markfysikaliska undersökningar i odlad jord. XXII. Om de vattenhallande egenskaperna hos svenska jordar." *Grundförbättring*, 25, 53-243. (In Swedish)
- Beke, G.J., and MacCormick, M.J. (1985). "Predicting volumetric water retentions for subsoil materials from Colchester County, Nova Scotia." *Can. J. Soil Sci.*, 65, 233-236.
- Brooks, R.H., and Corey, A.T. (1964). *Hydraulic properties of porous medium*. Hydrology Paper No. 3, Civil Engineering Department, Colorado State Univ., Fort Collins, Colo, USA.
- Dashtaki, S.G., Homae, M., and Khodaverdilo, H. (2010). "Derivation and validation of pedotransfer functions for estimating soil water retention curve using a variety of soil data." *Soil Use. Manage.*, 26, 68-74.
- Dijkerman, J.C. (1988). "An Ustult-Aguult-Tropept catena in Sirerra Leone, West Africa. II. Land qualities and land evaluation." *Geoderma*, 42, 29-49.
- Gupta, S.C., and Larson, W.E. (1979). "Estimating soil water retention characteristics from particle size distribution, organic matter percent, and bulk density." *Water Resour. Res.*, 15, 1633-1635.
- Fredlund, D.G., and Xing A. (1994). "Equations for the soil-water characteristic curve." *Can. Geotech. J.*, 31, 521-532.
- Hall, D.G.M., Reeve, M.J., Thomasson, A.I., and Wright, V.F. (1977). "Water retention, porosity and density of field soils." *Soil Survey*. Technical Monograph 9. Rothamsted Experimental Station, Lawes Agriculture Trust, Harpenden, UK.
- Jauhiainen, M. (2004). "Relationships of particles size distribution curve, soil water retention curve and unsaturated hydraulic conductivity and their implications on water balance of forest and agricultural hillslopes." *PhD Thesis*, Helsinki University of Technology, Espoo, Finland.
- Manrique, L.A., Jones, C.A., and Dyke, P.T. (1991). "Predicting soil water retention characteristics from soil physical and chemical properties." *Commun. Soil Sci. Plant Anal.*, 17, 1847-1860.
- Minasny, B., McBratney, A.B., and Bristow, K.L. (1999). "Comparison of different approaches to the development of pedotransfer functions for water-retention curves." *Geoderma*, 93, 225-253.
- Nemes, A., Schaap, M.G., Leij, F.J., and Wosten, J.H.M. (2001). "Description of the unsaturated soil hydraulic database UNSODA version 2.0." *J. Hydrol.*, 251, 151-162.
- Rajkai, K., and Varallyay, G. (1992). "Estimating soil water retention from simpler properties by regression technique." *Proc. International Workshop on Indirect Methods for Estimating the Hydraulic Properties of Unsaturated Soils*, M. Th. van Genuchten, ed., University of California, Riverside, CA, USA, 417-426.

- Rawls, W.J., Brakenseik, D.L., and Saxton, K.E. (1982). "Estimation of soil water properties." *Trans. ASAE*, 25, 1316-1320.
- Reichert, J.M., Albuquerque, J.A., Kaiser, D.R., Urach, F.L., and Carlesso, R. (2009). "Estimation of water retention and availability in soil of Rio Grande Do Sul." *Rev. Bras. Ciênc. Solo.*, 33, 1547-1560. (In Portuguese).
- Tomasella, J., and Hodnett, M.G. (1998). "Estimating soil water retention characteristics from limited data in Brazilian Amazonia." *Soil Sci.*, 163, 190-202.
- Van Genuchten, M.Th. (1980). "A closed-form equation for predicting the hydraulic conductivity of unsaturated soils." *Soil Sci. Soc. Am. J.*, 44, 892-898.

Examination of Capillary Regime in the Soil Water Retention Curve Using Multi-Phase Lattice Boltzmann Method

Jonathan F. Fili¹; Farshid Vahedifard²; Bohumir Jelinek³; and John F. Peters⁴

¹Graduate Student, Dept. of Civil and Environmental Engineering and Center for Advanced Vehicular Systems, Mississippi State Univ., Mississippi State, MS 39762. E-mail: jfili@cavs.msstate.edu

²Associate Professor, Dept. of Civil and Environmental Engineering, Mississippi State Univ., Mississippi State, MS 39762. E-mail: farshid@cee.msstate.edu

³Assistant Research Professor, Center for Advanced Vehicular Systems, Mississippi State Univ., Mississippi State, MS 39762. E-mail: bj48@cavs.msstate.edu

⁴Associate Research Professor, Center for Advanced Vehicular Systems, Mississippi State Univ., Mississippi State, MS 39762. E-mail: john@cavs.msstate.edu

Abstract

The soil water retention curve (SWRC) is a key constitutive relationship describing the behavior of variably saturated soils. Further insight into this behavior can be gained by studying the role of capillarity on pore adsorption. In this study, we employed a multi-phase lattice Boltzmann method (LBM) to investigate the effects of initial fluid density distribution on the capillary response of the system. The multi-phase LBM model was first validated against benchmark problems and was then employed to simulate a static particle array. The SWRCs were generated by recording the liquid pore pressure and the degree of saturation within a porous medium subjected to imbibition for two cases of initial fluid density distribution: randomized fluid density simulation (non-unified wetting front) and droplet simulation (unified wetting front). The results showed that the unified nature of the wetting front has a direct influence on the magnitude of the peak capillary response of the soil skeleton. The multi-phase LBM method is shown to be a promising tool to characterize capillary regime in partially saturated porous media. This modeling tool can be considered for future multi-scale numerical studies of multi-phase flow within porous media.

INTRODUCTION

The Soil Water Retention Curve (SWRC) is a key constitutive relationship for describing the behavior of variably saturated soils. The principal experimental approach for geotechnical and groundwater applications is developing the SWRC under inhibition and drainage conditions. The retention curves obtained in such experiments stem from complicated interactions among the air, water and solid phases that are difficult to quantify experimentally, even using modern tomographic imaging technology. Numerical simulations can offer an effective supplement to physical experiments whereby the multiple interactions among phases can be quantified simultaneously.

The lattice Boltzmann method (LBM) is growing in popularity for modeling flow in granular soils and is particularly attractive when coupled with the discrete element method (DEM) (Cundall and Strack 1979), which adds the ability to quantify interparticle stress. One of the main advantages of using this method is the ease at which one can generate models representing processes and effects at the molecular scale such as those producing phase separation and immiscibility. Coupling the LBM model with the DEM model allows local determination of the interparticle and fluid-particle interactions, thus creating a trajectory to a constitutive micromechanical model of unsaturated soil. Successful examples of such a coupled DEM-LBM model have been presented recently in the geomechanical literature (e.g., Lomine et al. 2013, Sun et al., 2013, Han and Cundall 2013, Johnson et al. 2017a, 2017b).

Galindo-Torres et al. (2016) performed a study exploring the LBM behavior by numerically simulating the SWRC in a small volume as proposed by Schaap et al. (2007). They proposed that the numerical simulation of the SWRC is unreliable due to the sensitivity of the functions to variations in initially imposed fluid conditions.

The main objective of this work is to investigate the effects of initial fluid density distribution on the capillary response of the system. For this purpose, a multi-phase LBM is used and validated against benchmark problems. The model is then employed within a static particle array generated by the DEM to isolate the effects of initial density distribution. Two cases include a randomized fluid density simulation (non-unified wetting front) and a droplet simulation (unified wetting front). The static particle configurations in this study afford an opportunity to examine the capillary behavior and to quantify changes in capillary response stemming from the shape of the wetting front.

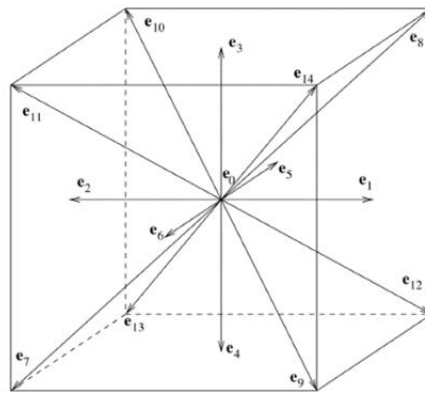


Figure 1. D3Q15 lattice velocities of the LBM

MULTI-PHASE LATTICE BOLTZMANN MODEL

The LBM models proposed by Shan and Chen (1993, 1994) (S-C) and Martys and Chen (1996) are used in the present study. These numerical representations are useful for modeling the SWRC because they model the liquid-vapor phase interface based on repulsive interactions between the fluid molecules themselves, independent of solid contacts and fluid-particle interaction. A multi-phase extension of LBM provides a valuable numerical model for soil specimens subjected to external forcing conditions (Schaap et al. 2007; Galindo-Torres et al. 2016).

Fluid cohesion

LBM models fluid cohesion in multi-phase flows by introducing interaction forces between the particles of fluid. The governing force on the fluid particles in absence of solid boundaries or obstacles is comprised solely of attractive (cohesive) forces between the fluid particles presented in Equation (1). The attractive force is based on an “interaction potential” ψ which is proportional to the density of fluid in a fluid cell under examination, as given by Equation (2).

$$F_a = -G_a \psi(x) \sum_{i=1}^{15} \omega_i \psi(x + \Delta t e_i) e_i \quad (1)$$

$$\psi = \psi_0 \exp\left(\frac{-\rho_0}{\rho}\right) \quad (2)$$

where G_a is a parameter representing strength of cohesive interaction, ω_i is the weighting coefficient for i^{th} direction (Equation 1), x is the lattice coordinate, Δt is the LBM timestep, e_i is the fluid velocity in the i^{th} direction as shown in Figure 1, and ψ_0 and ρ_0 are interaction potential parameters. (Equation 2) The sum is performed over all neighboring cells. Time evolution of a density in a single- phase LBM fluid is shown in Figure 3.

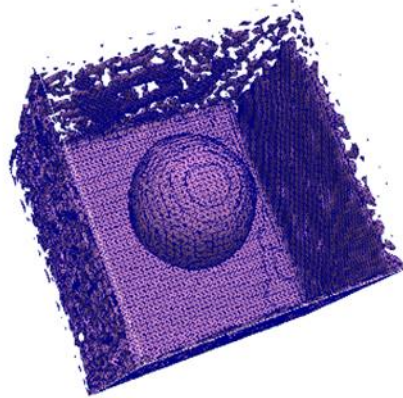


Figure 2. 3D single particle simulation showing the adhesion behavior of the fluid (purple) to the solid particle and to the solid walls of the specimen.

Fluid-solid interaction

In the presence of a solid boundary or particulate obstacle, the attractive (adhesive) force between the fluid and solid particles is given by

$$F_s = -G_s \psi(x) \sum_{i=1}^{15} \omega_i s(x + \Delta t e_i) e_i \quad (3)$$

following the same form as Equation (1), where s is a Boolean variable with respect the presence of solid in the LBM cell, and G_s is a parameter representing strength of adhesive interaction.

External force

An external force is incorporated as

$$F_g = \rho g \quad (4)$$

where g is a body force that is equivalent to the gravitational acceleration for a system in the gravitational field and ρ is the density of the fluid phase. After all contributing forces are added to the total force on a fluid particle, the velocity of the fluid particle is updated as follows

$$u' = u + \frac{\Delta t F}{\rho} \quad (5)$$

where u is the weighted fluid velocity given by Equation 7 and F is the total force on the fluid particle. Time evolution of a single-component 3D LBM system under gravity is shown in Figure 2.

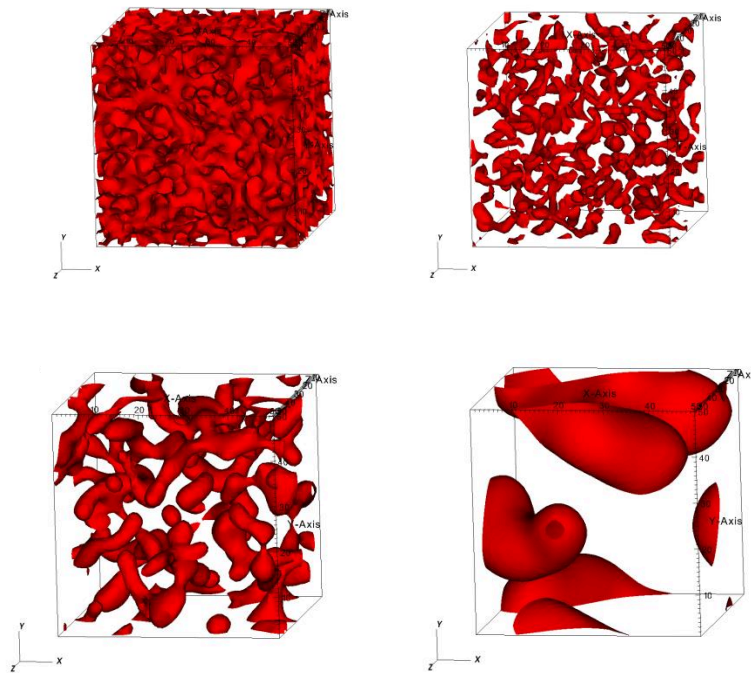


Figure 3. Simulation beginning with fluid density distribution randomized at initialization (red). As the simulation progresses, the intermolecular attractions of the fluid cause cohesion as shown.

Repulsion between two phases

A multi-phase fluid in the lattice Boltzmann model is represented by introducing additional density distribution for each additional fluid component. In case of a two-phase system, the densities of individual components are marked ρ_1 and ρ_2 . Each fluid component has its own G_a and G_s coefficients as described earlier by Equations (1) and (3). Furthermore, the two fluid components are also under the influence of a repulsive force:

$$F_r = -G_r \rho_1(x) \sum_{i=1}^{15} \omega_i \rho_2(x + \Delta t e_i) e_i \quad (6)$$

where strength of the repulsive interaction is characterized by a coefficient G_r . Total effective velocity of a mixture is calculated as a weighted sum of individual fluid velocities